Field Quality in Fermilab-built Models of Quadrupole Magnets for the LHC Interaction Regions

N. Andreev, T. Arkan, P. Bauer, R. Bossert, J. Brandt, D.R. Chichili, J. Carson, J. DiMarco, S. Feher, H. Glass, J. Kerby, M.J. Lamm, A. A. Makarov, A. Nobrega, I. Novitski, T. Ogitsu, D. Orris, J.P. Ozelis, T. Peterson, R. Rabehl, W. Robotham, G. Sabbi, P. Schlabach, C. Sylvester, J. Strait, M. Tartaglia, J.C. Tompkins, S. Yadav, A.V. Zlobin
Fermilab, Batavia, IL, USA
S. Caspi, D. McInturff, R. Scanlan
Lawrence Berkeley National Laboratory, Berkeley, CA, USA
A. Ghosh
Brookhaven National Laboratory, Upton, NY, USA

***Abstract*—Superconducting magnets for the interaction regions of the Large Hadron Collider are being developed by the US-LHC Accelerator Project. These 70 mm bore quadrupole magnets are intended to operate in superfluid helium at 1.9 K with a nominal field gradient of 215 T/m. The target field quality of the magnets is determined in collaboration with accelerator physics efforts within the US-LHC project and at CERN. A series of 2m model magnets are being built and tested at Fermilab to optimize design and construction parameters. Measurements of the field quality of the model magnets tested to date and comparisons with the required field quality are reported in this paper.**

I. Introduction

To achieve a luminosity of 10^{34} cm^{-2}s^{-1} at the LHC, special quadrupole magnets are required for the final focusing triplets in the interaction region [1]. These magnets must have sufficient cooling capacity to withstand the heavy heat load deposited by secondary particles from beam-beam collisions and provide a field gradient of 215 T/m over a 70 mm bore. High field quality is required due to large and rapidly varying values of the β-function. A design for these inner triplet quadrupoles has been developed by a Fermilab-LBNL collaboration (MQXB). Seven short models (HGQ01-HGQ07) of approximately 2m length have been fabricated. Six have been tested in superfluid helium at the Fermilab Vertical Magnet Test Facility. Field harmonics have been measured in the magnet straight section and in the end regions. In this paper we present the measurements and compare them with calculations based on as-built magnet geometry and with preliminary field quality specifications.

Manuscript received September 27, 1999.
Work supported by the U.S. Department of Energy.

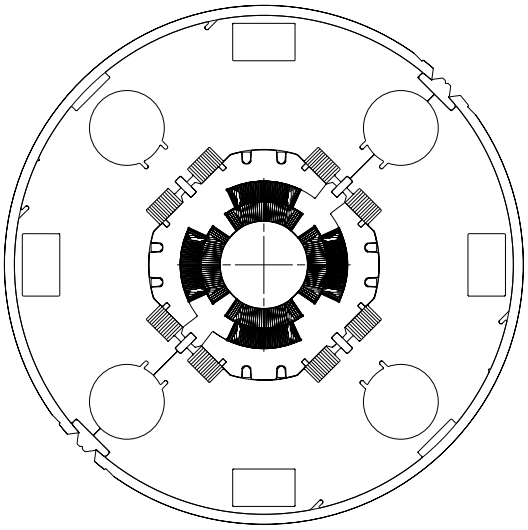

Fig. 1. Magnet cross-section.

II. MAGNET DESIGN

Figure 1 shows the magnet cross-section. The design is based on four two-layer coils connected in series, surrounded by collar and yoke laminations. No modifications to the design cross-section were made during the magnet model program, but various coil shimming schemes have been implemented in the models to obtain the desired coil modulus and prestress.

The end regions underwent several design iterations during the model program. The first five models were built with a four-block end configuration. With respect to the design of HGQ01, the second-wound group of the outer coil was shifted by 2 cm in the positive z direction starting with HGQ02 to reduce the peak field in the coil. A more compact design for the coil to coil joint in the lead end was introduced in HGQ03 and HGQ05. A new five-block configuration was implemented in models beginning with HGQ06 which improves the mechanical stability of inner layer conductors during winding. The new design also reduces the peak field in the coil and significantly

TABLE I
Reference collision harmonics for MQXB

n	$<b_n>$	$d(b_n)$	$\sigma(b_n)$	$<a_n>$	$d(a_n)$	$\sigma(a_n)$
Straight section (magnetic length 4.76/5.56 m)						
3	.0	.3	.8	.0	.3	.8
4	.0	.2	.8	.0	.2	.8
5	.0	.2	.3	.0	.2	.3
6	.0	.6	.6	.0	.05	.1
7	.0	.05	.06	.0	.04	.06
8	.0	.03	.05	.0	.03	.04
9	.0	.02	.03	.0	.02	.02
10	.0	.02	.03	.0	.02	.03
Lead end (magnetic length 0.41 m)						
2	-	-	-	40.	-	-
6	2.	2.	.8	.0	.5	.2
10	-.2	.2	.1	.0	.1	.1
Return end (magnetic length 0.33 m)						
6	.0	1.2	1.	-	-	-
10	-.25	.25	.1	-	-	-

improves field quality in the end region.

The model magnet collar design allows for use of tuning shims to correct field errors [2]. Shims are located in 8 rectangular cavities between the collars and yoke. In magnets HGQ01-05, these cavities were filled with a nominal shim package of half magnetic and half non-magnetic material. Thereafter, no shim package was inserted; the cavities were empty.

III. MEASUREMENT SYSTEM

Magnetic measurements presented in this paper were performed using a vertical drive, rotating coil system. Probes used have a tangential winding for measurement of higher order harmonics as well as specific dipole and quadrupole windings for measurement of the lowest order components of the field. These windings also allow for bucking the large dipole and quadrupole components in the main coil signal. Most measurements presented in this paper were made with a coil of 40.6 mm nominal diameter and length 82 cm. A short probe with 25 mm nominal diameter and 4.3 cm length was used for longitudinal scans of the magnet end region.

Coil winding voltages are read using HP3458 DVMs. An additional DVM is used to monitor magnet current. DVMs are triggered simultaneously by an angular encoder on the probe shaft, synchronizing measurements of field and current. Feed down of the quadrupole signal to the dipole is used to center the probe in the magnet.

IV. FIELD QUALITY ANALYSIS

In the straight section of the magnet, the field is represented in terms of harmonic coefficients defined by the power series expansion

$$B_y + iB_x = B_2 10^{-4} \sum_{n=1}^{\infty} (b_n + ia_n) \left(\frac{x+iy}{r_0} \right)^{n-1} \qquad (1)$$

where B_x and B_y are the transverse field components, B_2 is the quadrupole field strength, b_n and a_n are the $2n$-pole coefficients (b_2=10^4) at a reference radius r_o of 17 mm. The coordinate system for magnetic measurement is defined with the z axis at the center of the magnet aperture and pointing from return to lead end with the origin at the boundary between return end and straight section. The x axis is horizontal and pointing right, and the y axis, vertical and pointing up to the observer who faces the magnet lead end.

Table I shows the reference harmonics at collision for MQXB magnets (version 2.0). For each harmonic component, values of the mean, uncertainty in mean and standard deviation are listed. This table provides a reference for the discussion of field quality issues related to machine performance and IR systems layout during magnet development. The goal of the R&D phase is to converge on a set of numbers satisfying these requirements that can be adopted as a field quality specification for magnet production. Preliminary results of beam tracking studies aimed at evaluating the impact of magnet field errors on LHC dynamic aperture indicate that the values listed in Table I are acceptable from the machine performance standpoint [3].

Large values for both allowed and unallowed harmonics were measured in HGQ01 due to the thick coil shims (up to 450 μm) needed to obtain the required pre-stress, affecting b_6 and b_{10}, and differences in coil sizes (80 μm) in the different quadrants, producing a_4 and a_8. Significant improvements have been made in fabrication procedures. Coil shim thickness have been reduced and better uniformity in coil size and modulus has been achieved which has led to corresponding improvement in field quality from magnet to magnet. Table II shows a comparison between measured harmonics and calculations based on as-built parameters for the harmonic components b_6, b_{10}, a_4 and a_8. Calculations and measurements are generally in good agreement. The measurements are made at a current of 6 kA where all non-geometric components (conductor magnetization, iron saturation, conductor displacement under Lorentz forces) are small. A reduction of the errors of about one order of magnitude is observed from magnet HGQ01 to magnet HGQ05. In magnets HGQ05, all four harmonics are within the uncertainties specified by the reference table. Calculated values for these components of the field based on as-built parameters are similarly small in HGQ06 and HGQ07.

Table III shows the measured straight section harmonics up to the 20-pole for all models. In magnets HGQ05-7, all central harmonics are within one standard deviation of the random error specified in Table I. From the values in Table III, averages and standard deviations over the six models have been obtained for each component (Table IV). In the attempt to eliminate the effect of systematic errors due to coil shims, the values for b_6, b_{10}, a_4 and a_8 in Table IV have been obtained after taking the difference between measured values and those calculated based on as-built parameters (Table II). All average values and standard deviations in Table IV are within the limits spec-

TABLE II

Comparison of measured straight section harmonics (6 kA) with calculations based on as-built parameters.

n	HGQ			
	01	02	03	05
b_6, calc.	-4.24	-2.86	-1.39	-0.08
b_6, meas.	-3.91	-1.54	-1.02	-0.30
b_{10}, calc.	-0.14	-0.09	-0.04	0.01
b_{10}, meas.	-0.10	-0.10	-0.04	0.01
a_4, calc.	1.27	0.94	0.00	0.00
a_4, meas.	2.00	0.53	0.32	0.19
a_8, calc.	0.02	0.00	0.00	0.00
a_8, meas.	0.02	0.02	0.03	0.00

TABLE III

Measured harmonics in the magnet straight section (6 kA).

n	HGQ					
	01	02	03	05	06	07
b_3	0.36	-0.70	1.04	0.72	0.25	0.18
b_4	0.26	0.18	0.14	0.00	0.09	0.01
b_5	-0.29	0.09	-0.34	-0.04	-0.11	-0.04
b_6	-3.91	-1.54	-1.02	-0.30	-0.05	-0.45
b_7	-0.08	-0.01	-0.06	0.01	-0.03	0.017
b_8	0.06	0.01	0.00	0.00	0.00	0.00
b_9	0.04	0.00	0.00	0.00	0.00	-0.01
b_{10}	-0.10	-0.10	-0.04	0.01	0.00	-0.02
a_3	0.27	0.55	-0.30	0.12	-0.27	0.41
a_4	2.00	0.53	0.32	0.19	-0.31	-0.50
a_5	0.02	-0.17	0.26	0.05	-0.07	-0.24
a_6	-0.08	0.03	0.07	-0.03	-0.05	-0.10
a_7	-0.05	0.00	-0.03	0.01	0.00	0.07
a_8	0.02	0.02	0.03	0.00	0.00	0.01
a_9	0.01	-0.01	0.01	0.00	0.00	0.01
a_{10}	0.02	0.00	-0.01	0.00	0.00	0.00

ified in Table I. Note the b_6 result is strongly influenced by the relatively large difference between calculation and measurements in a single magnet (HGQ02). Moreover, one can expect smaller variations in a magnet production series than those observed in the first few models of a new design.

The magnet design provides good compensation of the saturation and Lorentz force effect, and the change in the average harmonic value between injection and operating current is very small. In particular, the 6 kA measurements (Table III) do not differ significantly from those taken at higher currents. The difference between harmonics measured during down and up ramp was small in

TABLE IV

Average and standard deviation of harmonics

n	$<b_n>$	$\sigma(b_n)$	$<a_n>$	$\sigma(a_n)$
3	0.31	0.59	0.13	0.35
4	0.11	0.10	0.00	0.49
5	-0.12	0.16	-0.03	0.18
6	0.20	0.64	-0.02	0.06
7	-0.03	0.04	0.00	0.04
8	0.01	0.02	0.01	0.01
9	0.01	0.02	0.00	0.01
10	0.00	0.02	0.00	0.01

TABLE V

Difference between field harmonics measured on the up and down ramp in HGQ06 (6 kA)

	10 A/s		80 A/s	
n	Δb_n	Δa_n	Δb_n	Δa_n
3	-0.94	-0.43	-6.67	-3.57
4	-0.16	-0.03	-1.19	0.11
5	0.12	0.11	0.86	0.61
6	0.20	-0.03	2.07	-0.23
7	-0.04	-0.01	-0.27	-0.11
8	0.00	0.00	0.00	0.00
9	0.01	0.00	0.06	-0.02
10	-0.01	0.00	-0.06	-0.02

magnets HGQ01-5, indicating small magnetization and eddy current effects [4]. However, in magnets HGQ06 and HGQ07, large differences between harmonics measured during up and down ramps were seen. These differences increased with increasing ramp rate (Table V). These ramp rate dependent field effects are due to eddy currents in the magnet coils. Effects seen in the measured fields for these two magnets are consistent with measurements of energy losses during AC cycling of magnet power [5]. We believe the eddy currents are due to low and varying crossover resistances in the coils of these magnets caused by changes in the coil curing temperature and pressure. In particular, magnets HGQ06 and 07 were the only ones in which the coils were cured at both high temperature (190°C) and pressure (Table VI). Predictions for crossover resistance values based on the measured harmonics for HGQ06 are plotted in Figure 2 and show low resistance values and large variations from coil to coil.

TABLE VI

Coil curing cycle

	coil curing cycle		I_c	$\Delta b_6, 6kA$
	temperature	pressure	300 A/s	40 A/s
HGQ01	135°	low	10965	0.02
HGQ02	190°	low	11335	0.21
HGQ03	195°	low	11298	0.16
HGQ05	130°	low	10519	0.12
HGQ06	195°	high	6433	-1.04
HGQ07	195°	high	4487	-0.55

Magnetic measurements of the HGQ06 lead end have been performed at a sequence of positions along the z axis, in steps of 4.3 cm to match the winding length. Due to the presence of a longitudinal field component, and to the dependence of the transfer function on the longitudinal position, the local end field is best described in terms of field integrals over the probe length, at the probe radius. A comparison between calculated and measured B_2 is shown in Fig. 3.

In the magnet end regions, additional terms (pseudo-multipoles) are required in the harmonic expansion for the local field. A simple expansion based on Equation 1 can however be applied to the total integral of the transverse field across the end region [6]. As in the magnet straight section, the integrated multipole components in the end

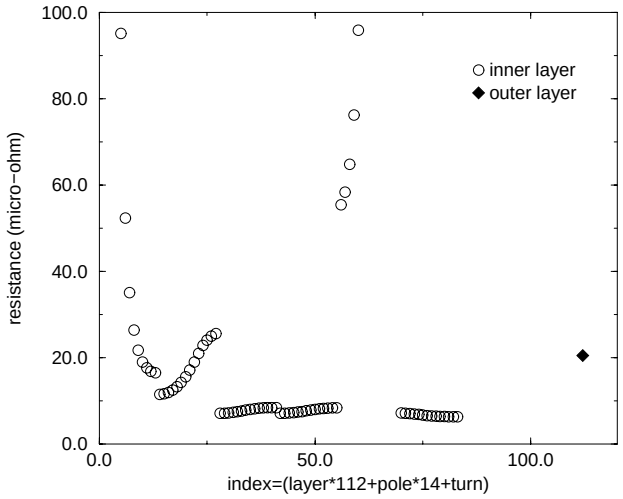

Fig. 2. Crossover resistance (HGQ06)

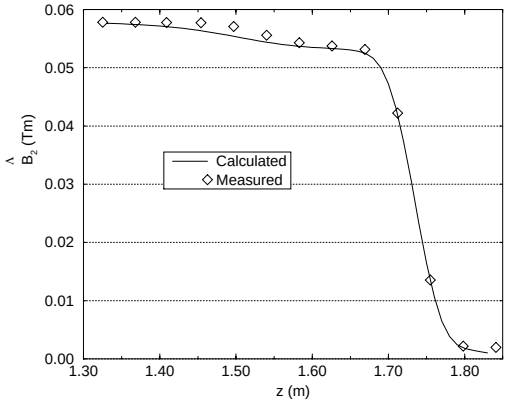

Fig. 3. Normal quadrupole in HGQ06 lead end.

regions are expressed in units of 10^{-4} of the main integrated quadrupole field. The magnetic length L_m of the interval is defined as the length of straight section which would provide an equivalent integrated gradient. The reference integration interval in z for harmonic coefficients in the magnet ends is defined to be [-0.57, 0.25] m for the return end and [1.31, 2.13] m for the lead end, matching the length of the measurement probe.

A comparison of measured and calculated harmonics in the magnet lead end is given in Table VII [1]. Harmonics are calculated using the program ROXIE [7]. For magnet HGQ02 and HGQ03, which used soft ULTEM end parts, thick mid-plane shims were applied to reach the desired pre-stress, resulting in a negative contribution to the dodecapole. In HGQ05, which uses G10 end parts, the thickness of the end shims was substantially reduced. This change in end shims, together with the reduction of the negative contribution from the straight section b_6,

[1] Except for HGQ01, for which a correction of -2 units was applied to the calculated b_6 integral for HGQ01 to include the contribution of mid-plane shims, the end harmonics quoted in Table VII are computed for the design geometry without considering the effect of coil shims.

TABLE VII
Calculated/measured harmonics in lead end.

n	HGQ					
	01	02	03	05	06	07
b_6, calc.	3.1	5.5	5.4	5.4	3.5	3.5
b_6, meas.	2.9	4.2	3.8	8.0	3.1	3.1
b_{10}, calc.	-0.3	-0.3	-0.4	-0.4	-0.1	-0.1
b_{10}, meas.	-0.3	-0.2	-0.4	-0.2	-0.1	-0.1
a_6, calc.	0.5	0.4	-0.1	-0.1	-0.7	-0.7
a_6, meas.	0.1	0.2	-0.3	-0.6	-0.4	-0.3
a_{10}, calc.	-0.1	0.0	0.0	0.0	0.0	0.0
a_{10}, meas.	-0.1	0.0	0.0	0.0	0.0	0.0

contributes to the positive jump in the measured dodecapole of HGQ05 with respect to HGQ03. Although the present lead end b_6 is larger than specified in the table of reference harmonics, a reduction of its systematic value by about 30% was achieved with the new 5-block end design.

V. Conclusions

Magnetic measurements of MQXB short models confirm design calculations for geometric harmonics, magnetization and Lorentz force effects. Refinements in magnet fabrication have significantly improved the field quality in the last three magnets which have systematic and random values of the harmonics in the straight section that are within specifications. The systematic normal dodecapole in the lead end is presently larger than the value listed in Table I, but a significant improvement was achieved after implementation of a new 5-block design. Current-dependent effects measured in early magnets were small, but large eddy current effects have been observed in HGQ06 and 07 due to changes in coil curing parameters.

References

[1] "LHC Conceptual Design", CERN AC/95-05 (LHC).
[2] G. Sabbi, et. al., "Correction of High Gradient Quadrupole Harmonics with Magnetic Shims", this conference.
[3] J. Wei, et al., 1999 Particle Accelerator Conference, New York, April 1999.
[4] N. Andreev, et. al., "Field Quality of Quadrupole R&D Models for the LHC IR", 1999 Particle Accelerator Conference, New York, April 1999.
[5] N. Andreev, et. al., "Quench Behavior of Quadrupole Model Magnets for the LHC Inner Triplets at Fermilab", this conference.
[6] G. Sabbi, et. al., "Magnetic Field Analysis of the First Short Models of a High Gradient QUadrupole for the LHC Interaction Regions", Proc. MT-15 Conf., Beijing, 1997.
[7] S. Russenschuck, Proc. ACES Symposium, Monterey, 1995.